

Bearing Capacity of L-shaped Latticed Joints Connected by Welding of Screw-fitted Dowels

Xudong Zhu,^{a,b,c} Yingying Xue,^a Pengfei Qi,^a Qian Lan,^a Liang Qian,^a Jie Shen,^a Ying Gao,^d Jiajia Li,^a Changtong Mei,^c and Shengcai Li^{b,*}

Three kinds of L-shaped latticed joint were designed to study the shear bearing capacity of joints prepared by welding of wooden dowels prepared with self-tapping screws. The results showed that such composite dowels in all specimens showed varying degrees of bending and splitting on the surface of the beech dowel after the shear test. The bending bearing capacity of the joint was the bending moment at the geometric center of the four composite dowels. The shear force of each composite dowel generated from the bending moment was equal with the same direction. The ultimate standard value of the theoretical loading force (F) was equal to 4.44 kN and the calculated design value (F_d) was equal to 2.96 kN. The errors between the standard and design value and test value of 3.94 kN were 11.2% and 24.9%, respectively. The theoretical value was relatively consistent with the test value. If the calculated design value was applied to estimate the ultimate bearing capacity of the joint, it was on the conservative side.

DOI: 10.15376/biores.18.1.949-959

Keywords: Bearing capacity; L-shaped latticed joint; Composite dowel welding

Contact information: a: Yangzhou Polytechnic Institute, Yangzhou University, Jiangsu 225100, China; b: College of Building Science and Engineering, Yangzhou Polytechnic Institute, Jiangsu 225100, China; c: Nanjing Forestry University, Nanjing 210018, China; d: Beijing Forestry University, Beijing 100035, China; * Corresponding author: li_shcai@126.com

INTRODUCTION

Wood dowel welding creates a new bonding interface layer through the friction between the wood dowels and substrate holes. During this process, some wood components are softened, fused, and eventually solidified until the friction stops (Leban *et al.* 2008).

Several researchers have studied the properties of the wood dowel welding joints, especially the pullout resistance. Belleville *et al.* (2011; 2013) and Auchet *et al.* (2010) studied the influence of the rotation and insert speed. In a previous study, the rotational speed of 2,400 revolutions per minute (rpm) and an insert speed 10 mm/s was the best choice for birch dowel and larch substrate (Zhu *et al.* 2019). However, Leban *et al.* (2008) found that the best rotational speed for beech dowels was 1,500 rpm. Belleville (*et al.* 2013) found that maple wood dowels could obtain a larger pullout resistance than beech dowels after welding. Meanwhile, black molten materials were mainly generated from wood dowels at the joint interfaces. According to the test result of the beech dowel welding with a rotational speed of 1,500 rpm, the pullout resistance of the beech dowel welding joint was 30% higher than that of the birch dowel (Xue *et al.* 2022). Other studies have reached the same conclusion that the wood dowel welding joint achieved the best pullout resistance when the diameter ratio of the wood dowel and the pre-drilled hole was approximately 1.25

(Kanazawa *et al.* 2005; Bocquet *et al.* 2007a; Zhu *et al.* 2017). Kanazawa *et al.* (2005) also found that dry wood dowel welding could promote the pullout resistance of the welding joint. Zhu *et al.* (2017) found that a wood dowel with a moisture content (MC) of 2% was the optimum condition.

Several studies have been conducted on the application of wood dowel welding due to its good pullout resistance and strong bonding properties. Girardon *et al.* (2014) studied the properties of a multi-layer beam connected by wood dowel welding. Bocquet *et al.* (2007b) designed a wood dowel welding cross laminated floor in which both the beam and the floor showed the basic properties, but with a lower rigidity than in the case of joints manufactured by the adhesive. On the other hand, in a study on the shear strength of the joint connected by wood dowel welding, the wood dowels were broken during the shear test with low displacement, even at 5 mm (Jia *et al.* 2022).

In a study by He *et al.* (2013), an innovative joint for timber structures, named a prestressed tube bolted joint with slotted-in steel plate, was designed to improve the low slip modulus of bolted joints. Different from bolted joints, the innovative joints resisted the slip of steel plate by the friction between the steel plate and the tubes, which were inserted into timber holes tightly and prestressed by a pretensioned bolt. Loading tests of single innovative joints and single bolted joints in tension were conducted, which indicated that single innovative joints outperformed single bolted joints in load-bearing capacity and slip modulus. The ductility of innovative joints was also desirable if the load was controlled. According to the properties and performance of wood dowel and self-tapping screw, a new beech and self-tapping screw composite dowel was designed in a study by Xue *et al.* (2022). Other studies have examined the single shear performance (Qian *et al.* 2022; Zhu *et al.* 2022).

To investigate the rotational behavior of a bolted glulam connection with slotted-in steel plates under pure bending and combined shear and bending, and establish the moment resistance calculation model, based on the resistance of single bolted connection loaded perpendicular to wood grain, monotonic loading test was carried out. The test results indicated that all connections fail due to perpendicular to wood grain splitting (Wang *et al.* 2016). The simplified calculation method of a bolted glulam connection was found to be an optimum choice for the studied conditions. On the other hand, a force analysis of the connection under shear forces and bending moment was proposed by Porteous and Kermani (2007). Furthermore, this method was applied to analyze the force of the beam-to-column connection by Li *et al.* (2021).

This study investigated the latticed beam-to-column joint connected by composite dowels prepared with self-tapping screws and rotational welding. This system presented a double shear mode. Without considering the extrusion between the beam-end and the pillar-side, the joint was simplified to an L-shaped joint made of vertical spruce-pine-fir (SPF) on both sides and a transversal SPF in the middle. Such an arrangement can be approximately regarded as a model that is rotated around the geometric center of the connection group. Based on this model, the bearing capacity was studied in this paper.

EXPERIMENTAL

Materials

Wood dowels were prepared from *Zelkova schneideriana* beech wood (Crownhomes, Jiangsu, China). The wood dowels were 12 mm in diameter and 120 mm in

length. The density of the dowels was 703 kg/m^3 and the MC was 2%. The mechanical properties of the wood dowels are presented in Table 1.

Table 1. The Mechanical Properties of the Wood Dowels

Size (mm)	Tensile Force (kN)	Bending Strength (MPa)	Elastic Modulus (MPa)
12 × 120	6.31 (0.17) ¹	93.68 (8.07)	9,862 (432.87)

¹-Values in parentheses are standard deviations

The self-tapping screws (STSs) (Moregood, Shanghai, China) that were utilized in this study had a diameter of 6 mm and a length of 120 mm. The inner diameter of the thread was 4.0 mm. The diameters of the rod and head were 4.3 mm and 12 mm, respectively. The surface of the STSs was galvanized. The characteristic values of the bending and tensile strength were 1,000 and 1,100 MPa, respectively.

The substrate material was grade II SPF (Crownhomes, Jiangsu, China). The SPF material had dimensions of 89 mm (width) × 38 mm (thickness) × 500 mm (length). The density was 495 kg/m^3 and the MC was 9.7%. The composite dowels were made using a two-step procedure. First, a hole was drilled in the middle of the beech dowel along the length. The size of the hole was 3.5 mm in diameter and 120 mm in depth. A drilling machine (TBH Type 28 124; Proxxon, Stuttgart, Germany) was used in this procedure. Second, the STS was screwed into the pre-drilled hole in the middle of the beech dowel (Fig. 1).

Experimental Design

Specimen prepared

The composite dowels were welded into the pre-drilled holes by a high-speed rotation of 1,500 rpm without cutting any off. The substrates were connected by two connectors parallel (Group A) and vertical (Group B) to the loading direction, as can be seen in Figs. 2 and 3, respectively. The substrates that were connected by four connectors (Group C) is shown in Fig. 4. Six specimens were prepared for all the three kinds of L-shaped latticed joint groups. All the specimens were conditioned to an equilibrium MC of 12% at a temperature of 20 °C and a relative humidity (RH) of 65%.



Fig. 1. An image of the composite dowel

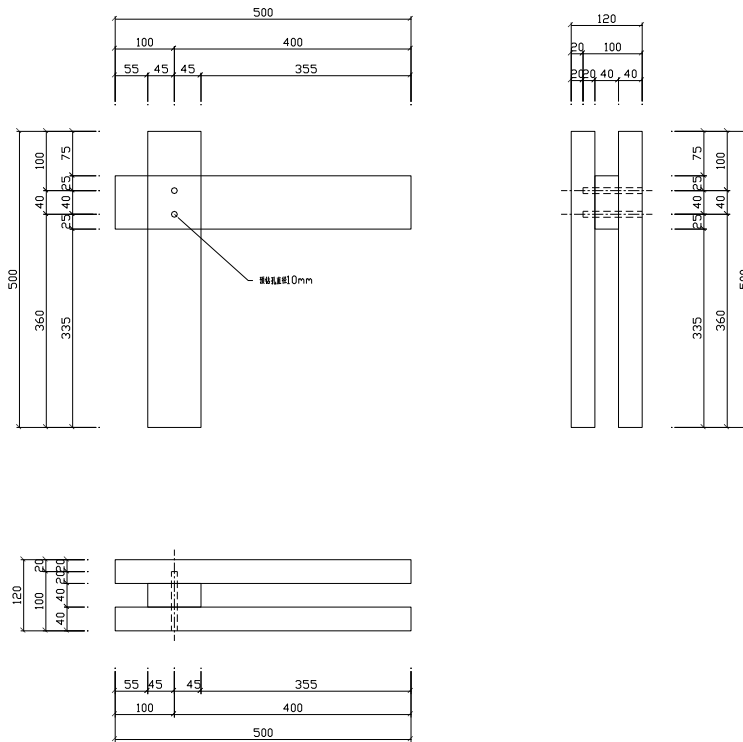


Fig. 2. Diagram of the substrates connected by one or two connectors parallel to the loading direction

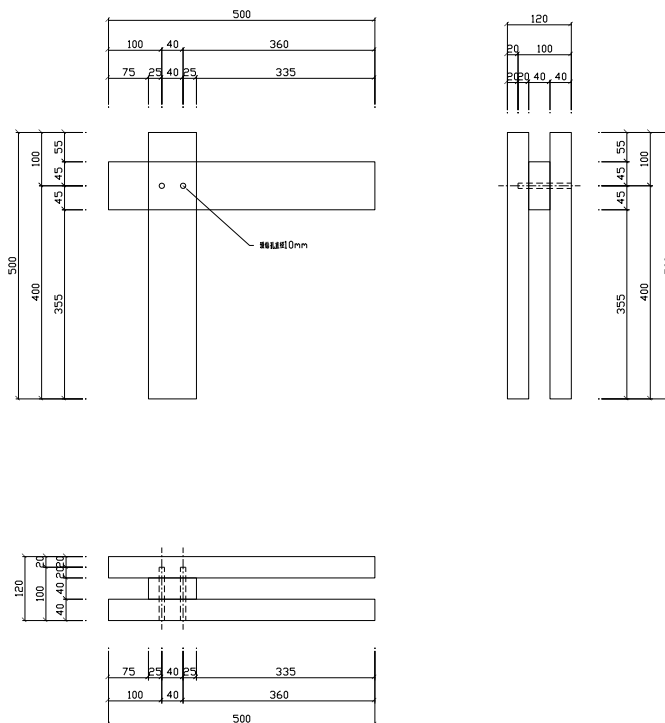


Fig. 3. Diagram of the substrates connected by one or two connectors vertical to the loading direction

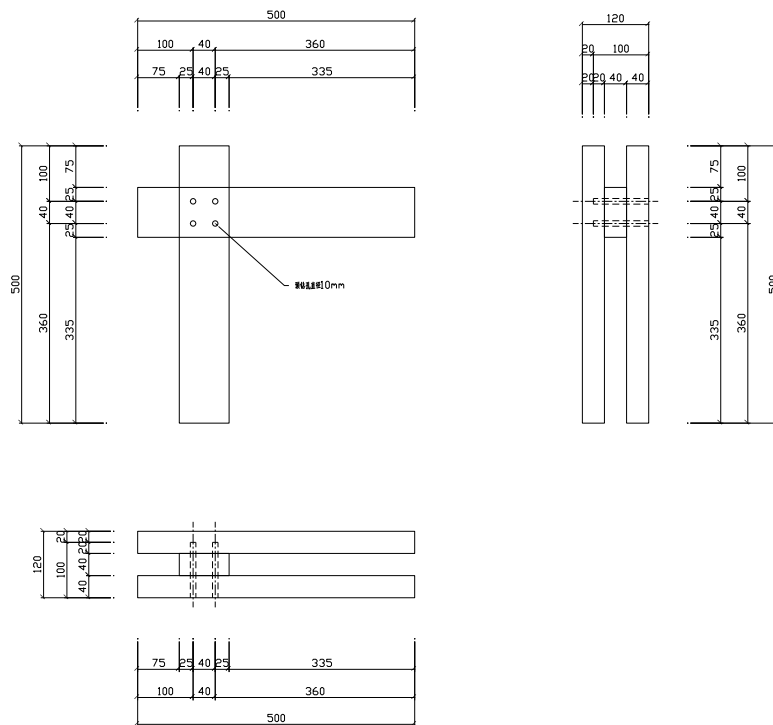


Fig. 4. Diagram of the substrates connected by four connectors

Lateral load resistance test

The universal testing machine (WDW-300E; Jinan Popwil, Jinan, China) was used to test the single shear properties, as can be seen in Fig. 5. The traction speed was 5 mm/min.



Fig. 5. Testing setup using the WDW-300E universal testing machine

RESULTS AND DISCUSSION

Experimental Phenomena and Failure Modes

As shown in Fig. 6, the damage pattern in Group A showed that one side of the vertical SPF specimens was cracked. In Group B, five specimens had splits in the middle transversal SPF specimen. One specimen did not show any obvious damage, but the bearing capacity started to decrease. In Group C, two specimens had splits in one side of the vertical SPF specimens, three specimens had splits in the middle transversal SPF specimen, and one specimen had splits in both vertical and vertical SPF specimen. The composite dowels in all three groups A, B, and C, showed varying degrees of bending and splitting on the surface of the beech dowel (Fig. 7).

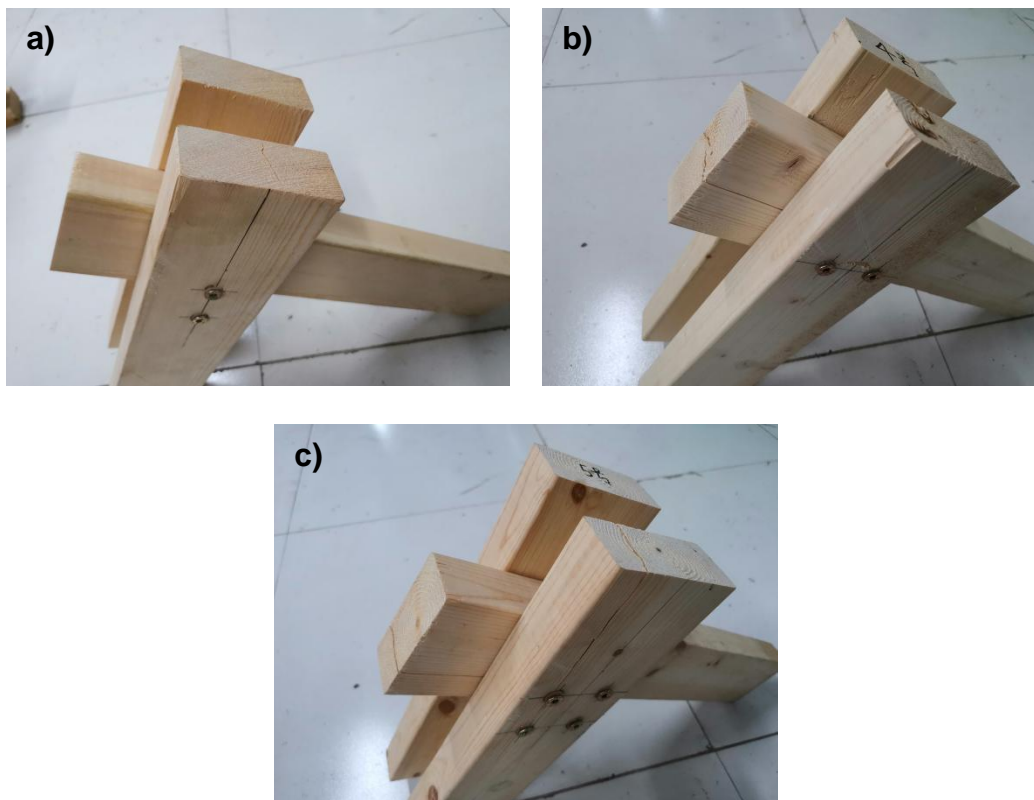


Fig. 6. Failure mode of the specimens from groups a) A, b) B, and c) C



Fig. 7. Failure mode of composite dowels

As can be seen in Table 2, the bearing capacity of the specimens in group A was similar to that of the specimens in group B. However, the bearing capacity of the specimens in group C was 2.6 times higher than the specimens in group A and group B. Based on these test values, during the test process, the shear force and bending moment were evenly distributed in the four composite dowels.

Table 2. The Test Values of the Specimens

Number	Group A (kN)	Group B (kN)	Group C (kN)
1	1.26	1.35	3.74
2	1.35	1.68	4.16
3	1.41	1.41	3.56
4	1.23	1.75	4.26
5	1.10	1.22	3.53
6	1.05	1.62	4.39
The mean value	1.23	1.51	3.94
Standard deviation	0.14	0.21	0.38

Calculation Method of the Ultimate Bearing Capacity

In this study, the bearing capacity of the joints connected by four composite dowels were calculated. According to a previous study (Xue *et al.* 2022), the pullout resistance of one composite dowel was 6.10 kN. The single shear force of the joints connected by one and four composite dowels was calculated to be 4.82 and 17.6 kN, respectively.

Porteous *et al.* (2007) proposed a model for calculating the bearing capacity of the joint under the action of bending and shearing compound force. The shear force of the joint area was equally distributed to each composite dowel. The horizontal shear force (F_H) of each composite dowel was equal to H/n , the vertical shear force (F_V) was equal to V/n , and n was the number of composite dowels. The shear force (F_M) of each composite dowel created by the joint bending moment was perpendicular to the line between the composite dowels and the center of rotation. The F_M value was proportional to the distance between the composite and the center of rotation. The final shear force of the composite dowel under the coupling action of bending and shearing force was the vector sum of the F_H , F_V , and F_M values.

As shown in Fig. 6, two vertical SPF specimens were used as column components, and one horizontal SPF specimen was used as the beam component. After the joint reached to the maximum load-bearing capacity, the three specimens were split and the displacement was increased. To simplify the analysis process and the calculated model, the split effect of the column was ignored. The rotational performance of the end of the beam was considered in the calculated process. For the joint connected by four composite dowels in this paper, a concentrated load (F) was applied to the beam at a distance of 250 mm from the geometric center of the joint (Fig. 8). Then, the bending moment (M) and F_M were acted on the composite dowels. From Fig. 8, the geometric center of the joint was the center of rotation. The bending moment and shear force were calculated according to Eq. 1,

$$M = 0.25F \quad (1)$$

where M is the bending moment (kN·m), and F is the concentrated load (kN).

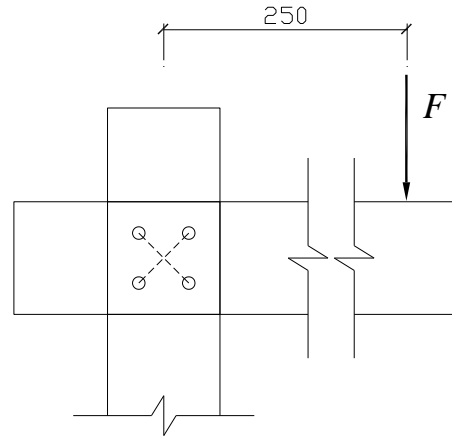


Fig. 8. Sketch map of the load applied in the joint

The simple sketch map of the joint is shown in Fig. 9. The bending bearing capacity of the joint was the bending moment at the geometric center of the four composite dowels. The shear force of each composite dowel generated from the bending moment was equal with the same direction.

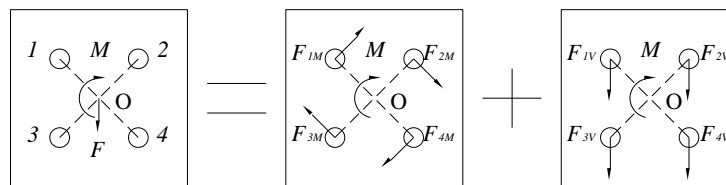


Fig. 9. Sketch map of the bearing capacity of the joint

When the bending moment acted alone on the composite dowels of the joint, Eq. 2 could be derived from the balance of the moment of force.

$$M = \sum_i^n F_{iM} r_i \quad (2)$$

Where F_{iM} is the shear force caused by the bending moment from the composite dowels of the joint, r_i is the distance between the center of the i composite dowel and the geometric center of the four composite dowels, and n is the number of the composite dowels.

When the shear force was applied individually to the joint, all the four composite dowels of the joint bore the force equally. The resisting shear force (F_{iV}) was generated from each composite dowel according to Eq. 3,

$$F_{iV} = \frac{F}{n} \quad (3)$$

The four composite dowels were arranged by a square shape. The distance between each composite dowel and the rotation geometric center of the joint was 34.65 mm. All the four composite dowels bore the F_{iM} and F_{iV} . The F_{iM} of each composite dowel was the same amount with different directions. The each F_{iV} was the same amount and direction. The combined force F_i was composed of the F_{iM} and F_{iV} values. The angle θ between the F_i and the grain direction was calculated using Eq. 4,

$$\theta_i = \arctan \left(\frac{F_{iM} \sin \alpha_i + F_{iV}}{F_{iM} \cos \alpha_i} \right) \quad (4)$$

where α_i is the angle between bearing capacity of the shear surface of the i composite dowel and the grain direction (45°).

In examining the second composite dowel in Fig. 9, the θ_2 , F_{2M} , F_{2V} , and F_2 values were 50.1° , 8.01 kN, 1.21 kN, and 8.82 kN, respectively.

The ultimate standard value of the theoretical loading force (F) was equal to 4.44 kN and the calculated design value (F_d) was equal to 2.96 kN. The errors between the standard and design value and test value 3.94 kN were 11.2% and 24.9%, respectively. The theoretical value was relatively consistent with the test value. If the calculated design value was applied to estimate the ultimate bearing capacity of the joint, it was on the conservative side.

CONCLUSIONS

1. The composite dowels prepared with beech wood and self-tapping screws in all three groups A, B, and C, including joints comprising two composite dowels and four composite dowels, showed varying degrees of bending and splitting on the surface of the beech dowel.
2. The bearing capacity of the joint was the bending moment at the geometric center of the four composite dowels. The shear force of each composite dowel generated from the bending moment was equal with the same direction.
3. The theoretical value was relatively consistent with the test value. If the calculated design value was applied to estimate the ultimate bearing capacity of the joint, it was on the conservative side.

ACKNOWLEDGMENTS

The authors are grateful for the support of the National Natural Science Foundation of China (Grant No. 31901252), the Jiangsu Planned Projects for Postdoctoral Research Funds (Grant No. 2020Z075), the Science and Technology Program of Jiangsu Housing and Construction Department (Grant No. 2020ZD39, 2021ZD22), the Qing Lan Project of Jiangsu, the Yangzhou Science and Technology Project (Grant No. YZ2020203, YZ2022110), and the Natural Science Foundation of the High Education Institutions of Jiangsu Province (Grant No. 22KJA220003). The authors thank TopEdit (www.topeditsci.com) for its linguistic assistance during the preparation of this manuscript.

REFERENCES

- Auchet, S., Segovia, C., Mansouri, H. R., Meausoone, P.-J., Pizzi, A., and Omrani, P. (2010). "Accelerating vs constant rate of insertion in wood dowel welding," *Journal of Adhesion Science and Technology* 24(7), 1319-1328. DOI: 10.1163/016942409X12598231568384

- Belleville, B., Ségovia, C., Pizzi, A., Stevanovic, T., and Cloutier, A. (2011). "Wood blockboards fabricated by rotational dowel welding," *Journal of Adhesion Science and Technology* 25(20), 2745-2753. DOI: 10.1163/016942410X537323
- Belleville, B., Stevanovic, T., Pizzi, A., Cloutier, A., and Blanchet, P. (2013). "Determination of optimal wood-dowel welding parameters for two North American hardwood species," *Journal of Adhesion Science and Technology* 27(5-6), 566-576. DOI: 10.1080/01694243.2012.687596
- Bocquet, J.-F., Pizzi, A., Despres, A., Mansouri, H. R., Resch, L., Michel, D., and Letort, F. (2007a). "Wood joints and laminated wood beams assembled by mechanically-welded wood dowels," *Journal of Adhesion Science and Technology* 21(3-4), 301-317. DOI: 10.1163/156856107780684585
- Bocquet, J.-F., Pizzi, A., and Resch, L. (2007b). "Full-scale industrial wood floor assembly and structures by welded-through dowels," *European Journal of Wood and Wood Products* 65(2), 149-155. DOI: 10.1007/s00107-006-0170-4
- Girardon, S., Barthram, C., Resch, L., Bocquet, J.-F., and Triboulot, P. (2014). "Determination of shearing stiffness parameters to design multi-layer spruce beams using welding-through wood dowels," *European Journal of Wood and Wood Products* 72(6), 721-733. DOI: 10.1007/s00107-014-0834-4
- He, M., Ni, S., Ma, R., and Bai, X. (2013). "Loading tests of prestressed tube bolted joint with slotted-in steel plate," *Journal of Tongji University* 41(9), 1353-1358. DOI: 10.3969/j.issn.0253-374x.2013.09.012
- Jia, H., Gao, Y., Meng, X., Yang, H., Zhang, Y., and Xu, F. y. (2022). "Shear tests and theoretical analysis of wood-dowel rotation welding joints," *Journal of Forestry Engineering* 7(1), 38-44. DOI: 10.13360/j.issn.2096-1359.202102007
- Kanazawa, F., Pizzi, A., Properzi, M., Delmotte, L., and Pichelin, F. (2005). "Parameters influencing wood-dowel welding by high-speed rotation," *Journal of Adhesion Science and Technology* 19(12), 1025-1038. DOI: 10.1163/156856105774382444
- Leban, J.-M., Mansouri, H. R., Omrani, P., and Pizzi, A. (2008). "Dependence of dowel welding on rotation rate," *European Journal of Wood and Wood Products* 66(3), 241-242. DOI: 10.1007/S00107-008-0228-6
- Li, Z., Luo, J., He, M., Yu, X., Liang, F., Shu, Z., and Sun, Y. (2021). "Analytical investigation into the rotational behavior of glulam bolted connections with slotted-in steel plated under coupled bending moment and shear force," *China Civil Engineering Journal* 54(3), 98-108. DOI: 10.15951/j.tmgcxb.2021.03.009
- Porteous, J., and Kermani, A. (2007). *Structural Timber Design to Eurocode 5*, Wiley-Blackwell, Hoboken, NJ, USA.
- Qian, L., Xue, Y., Shen, J., Gao, Y., Li, S., Gao, Y., Yao, L., Gong, Y., Wang, Z., Ding, Q., et al. (2022). "Analytical investigation into the single shear performance of a joint with a new beech and self-tapping screw composites dowel," *BioResources* 17(2), 2347-2357. DOI: 10.15376/biores.17.2.2347-2357
- Wang, M., Gu, X., Song, X., and Wu, Y. (2016). "Experimental study on bolted glued laminated timber connections with slotted-in steel plates under pure bending and combined shear and bending," *Journal of Building Structures* 37(4), 64-72. DOI: 10.14006/j.jzjgxb.2016.04.009
- Xue, Y., Zhu, X., Zhang, X., Qi, P., Li, J., Zhu, L. H., and Yao, L. (2022). "Single shear performance of components connected by beech-self-tapping-screw composite dowels," *Chinese Journal of Wood Science and Technology* 36(1), 68-74. DOI: 10.12326/j.2096-9694.2021037

- Zhu, X., Gao, Y., Yi, S., Ni, C., Zhang, J., and Luo, X. (2017). "Mechanics and pyrolysis analyses of rotation welding with pretreated wood dowels," *Journal of Wood Science* 63, 216-224. DOI: 10.1007/s10086-017-1617-4
- Zhu, X., Xue, Y., Shen, J., Huang, L., and Gao, Y. (2019). "Mechanism study on *Betula* wood dowel rotation welding into larch and enhanced mechanism of treating with CuCl_2 ," *BioResources* 14(4), 8785-8802. DOI: 10.15376/biores.14.4.8785-8802
- Zhu, X., Xue, Y., Zhang, X., Qi, P., Shen, J., and Mei, C. (2022). "Study of the single shear performance of a joint with a new beech and self-tapping screw composite dowel," *Journal of Renewable Materials* 10(2), 401-413. DOI: 10.32604/jrm.2022.016464

Article submitted: May 5, 2022; Peer review completed: October 1, 2022; Revised version received: November 5, 2022; Accepted: November 29, 2022; Published: December 7, 2022.

DOI: 10.15376/biores.18.1.949-959